

# SUPPLEMENTARY MATERIAL TO COMMUNICATION WITH MULTIPLE SENDERS: AN EXPERIMENT

EMANUEL VESPA AND ALISTAIR J. WILSON

## APPENDIX A. PROOFS OF CONSTRUCTION ON TORUS

**Proposition.** *A fully revealing perfect Bayesian equilibrium in the two-senders on two-circles cheap-talk game exists when: i) senders' biases satisfy  $\|\delta^X\|, \|\delta^Y\| < \sqrt{5} \cdot 45^\circ$ ; ii)  $\Delta$  has full rank and  $\delta^X \perp \delta^Y$ .*

*Proof.* Given the bias vector  $\Delta = [\delta^X \quad \delta^Y]$  define the normalized matrix  $\Gamma = [\gamma^X \quad \gamma^Y] := \begin{bmatrix} \frac{\delta^X}{\|\delta^X\|} & \frac{\delta^Y}{\|\delta^Y\|} \end{bmatrix}$ . We will examine the case where  $\gamma_1^Y, \gamma_2^Y, \gamma_2^X \geq 0$  and  $\gamma_1^X \leq 0$ , (where similar argument holds for other orthogonal vector directions, where we can simply change the positive direction, and/or relabel the coordinates). Define the clockwise angular measure

$$\phi(x) := \text{mod}(x, 360^\circ).$$

and the minor arc length (clockwise as positive) as

$$\phi_d(x) := \phi(x + 180^\circ) - 180^\circ,$$

where we let both functions act coordinate-by-coordinate on vectors. Let senders' message strategies be

$$\begin{aligned} \xi_X^*(\theta) &= \phi(\theta + \kappa_X \cdot \gamma^X), \\ \xi_Y^*(\theta) &= \phi(\theta + \kappa_Y \cdot \gamma^Y), \end{aligned}$$

where in general we could consider strategies to be mixtures over  $\kappa_X$  and  $\kappa_Y$ , however, for simplicity and to prove the best case for existence, let  $\kappa_X = \kappa_Y = 0$  on the path. Define the recommendation difference as  $\nabla(\mathbf{x}, \mathbf{y}) = \phi_d(\mathbf{y} - \mathbf{x})$ . The receiver's response to all message pairs  $\mathbf{x}, \mathbf{y} \in \Theta := [0, 360)^\circ$  is given by:

$$\zeta^*(\mathbf{x}, \mathbf{y}) = \phi\left(\mathbf{x} + \frac{1}{2}\nabla(\mathbf{x}, \mathbf{y}) - \Gamma \begin{bmatrix} -\frac{1}{2} & 0 \\ 0 & \frac{1}{2} \end{bmatrix} \Gamma^{-1}\nabla(\mathbf{x}, \mathbf{y})\right),$$

with corresponding beliefs that  $\theta = \zeta^*(\mathbf{x}, \mathbf{y})$  with certain probability for all  $\mathbf{x}, \mathbf{y}$  (per the paper's Proposition 1, except that the final choices are constrained to be on the circle here).

Along the path the arc length is always  $\nabla(\mathbf{x}, \mathbf{y}) = \mathbf{0}$  and the arc midpoint is the state,  $\mathbf{x} + \frac{1}{2}\nabla(\mathbf{x}, \mathbf{y}) = \theta$ , so the chosen point is  $\zeta^*(\xi_X^*(\theta), \xi_Y^*(\theta)) = \theta$ .<sup>1</sup> The receiver's reaction is therefore sequentially rational, and the on path beliefs are consistent, while all possible recommendations lead to an inferred point  $\zeta^*(\mathbf{x}, \mathbf{y}) \in \Theta$ .

---

*Date:* April, 2015.

<sup>1</sup>For mixed exaggeration strategies, this is also true so long as the distributions are chosen so that  $\kappa_Y\gamma^Y - \kappa_X\gamma^X \in (-180, 180)^\circ$ . A sufficient condition for this is that  $\kappa_X, \kappa_Y \in (-90^\circ, 90^\circ)$ .

What remains to be shown is that senders can not unilaterally deviate. Let sender  $X$  choose an arbitrary recommendation  $\mathbf{x} = \phi(\boldsymbol{\theta} + \tilde{\mathbf{x}}) \in \Theta$  where we take  $\tilde{x}_1, \tilde{x}_2 \in [-180^\circ, 180^\circ)$ , and  $Y$  follows the strategy. The final outcome is a point in the  $\gamma^Y$  direction from  $\boldsymbol{\theta}$  given by

$$\zeta^*(\boldsymbol{\theta} + \tilde{\mathbf{x}}, \boldsymbol{\theta}) = \phi(\boldsymbol{\theta} - (\gamma_2^X \tilde{x}_1 - \gamma_1^X \tilde{x}_2) \cdot \gamma^Y).$$

By orthogonality and unit length,  $|\gamma_i^X \gamma_i^Y| \leq \frac{1}{2}$ . Given the domains for  $\tilde{x}_1$  and  $\tilde{x}_2$ , the final choice can be located anywhere in  $\{\phi(\boldsymbol{\theta} + \lambda \cdot \gamma^Y) \mid \lambda \in (-180^\circ(\gamma_2^X - \gamma_1^X), 180^\circ(\gamma_2^X - \gamma_1^X))\}$ . The direction  $\gamma^Y$  locally separates  $X$ 's upper contour set, however, because of the circular topology, we need to make sure that it does so globally. We need to check that exaggerations cannot lead to an inference so far along the vector  $\gamma^Y$  that the response  $\zeta^*(\boldsymbol{\theta} + \tilde{\mathbf{x}}, \boldsymbol{\theta})$  gets close to  $\boldsymbol{\theta} + \boldsymbol{\delta}^X$  from the opposite direction, given cyclicity every  $360^\circ$  units. The condition then is that for all feasible  $\lambda$

$$\|\phi_d(\boldsymbol{\theta} + \lambda \cdot \gamma^Y - \boldsymbol{\delta}^X - \boldsymbol{\theta})\| \geq \|\phi_d(\boldsymbol{\theta} - \boldsymbol{\delta}^X - \boldsymbol{\theta})\|.$$

A sufficient condition for this is that bias has a magnitude  $\|\boldsymbol{\delta}^X\|$  smaller than  $\sqrt{5} \cdot 45^\circ$ .<sup>2</sup> The  $X$  sender is therefore indifferent over any exaggeration that satisfies  $(\gamma_2^X \tilde{x}_1 - \gamma_1^X \tilde{x}_2) = 0$ , but strictly prefers these points to any other.  $\square$

---

<sup>2</sup>This is the bias level at which a circle of radius  $\|\boldsymbol{\delta}^X\|$  centered at the point  $\begin{pmatrix} \theta_1 + \delta_1^X + 360^\circ \\ \theta_2 + \delta_2^X \end{pmatrix}$  touches the circle of radius  $180^\circ(\gamma_2^X - \gamma_1^X)$  centered at  $\boldsymbol{\theta}$ , which occurs when the coordinate system is rotated by  $\Psi = \arctan\{\sqrt{5} - 2\}$ . For different coordinate-system rotations this constraint on the biases will be slack.

## APPENDIX B. SENDER BEHAVIOR ANALYSIS

To examine *Sender Restriction B* and the subsequent *Equilibrium Restriction C*, we estimate the best-fitting exaggeration direction for sender  $X$  in each treatment, given by the unit length vector  $\gamma^X(\omega) := \begin{pmatrix} -\sin(\omega + \psi) & \cos(\omega + \psi) \end{pmatrix}'$ . The parameter  $\omega$  will be estimated, while  $\psi$  is the treatment rotation, so that estimates of  $\omega = 0$  indicate exaggerations in the bias-direction for  $X$ . For any specific exaggeration direction  $\gamma^X(\omega)$ , we can decompose an observed exaggeration  $\tilde{x}_{it}$  into the exaggeration in the  $\gamma^X(\omega)$ -direction ( $\kappa_{it}(\omega) = -\tilde{x}_{1it} \sin(\omega + \psi) + \tilde{x}_{2it} \cos(\omega + \psi)$ ), and a residual in the orthogonal direction ( $\epsilon_{it}(\omega) = \tilde{x}_{1it} \cos(\omega + \psi) + \tilde{x}_{2it} \sin(\omega + \psi)$ ). To estimate the best-fitting exaggeration direction, we find the  $\omega$  that minimizes.

$$Q(\omega; \psi) = \sum_{i,t} |\epsilon_{it}(\omega)| = \sum_{i,t} |\tilde{x}_{1it} \cos(\omega + \psi) + \tilde{x}_{2it} \sin(\omega + \psi)|.$$

So the estimated parameter  $\hat{\omega}$  minimizes the expected deviation from the chosen exaggeration direction. Together, *Sender Restriction B* and *Equilibrium Restriction C* imply no variation outside of a specific vector direction (so  $\min_{\omega} Q(\omega; \psi) = 0$ ) and that  $\omega = 0$ , respectively.

We pool exaggerations from subjects in both sender roles in each treatment and provide estimates for the exaggeration angle  $\hat{\omega}$ , and sample averages for the on-ray exaggeration  $\kappa_{it}(\hat{\omega})$  and the off-ray error size  $|\epsilon_{it}(\hat{\omega})|$  in Table SM-I.<sup>3</sup> The intuition suggested from Figure 4 in the paper clearly matches the estimates: the best-fit exaggeration directions are qualitatively close to the bias/equilibrium directions across all three treatments. In the case of R(1), the best-fit direction is significantly different from zero (at the 5 percent level), where the positive sign reflects exaggerations with a larger magnitude in issue 1 (the direction where the two senders have opposed biases) than issue 2 (where the senders have the aligned biases). However, from a quantitative point of view the difference with the equilibrium direction is small: the angle of the estimated exaggeration direction differs from the equilibrium by approximately  $\frac{\pi}{100}$  radians.

In addition to estimates for the exaggeration angle  $\omega$  at the aggregate level (the important variable for receivers given random matching), we also examined exaggerations at the subject-level, computing angle estimates  $\hat{\omega}_i$  using the same objective  $Q(\cdot)$  over the ten rounds each subject was a sender. Results from subject-level estimates are illustrated in Figure 4 in the paper as angular histograms in each plot, where we illustrate the estimated sender  $X$  direction  $\hat{\omega}_i + \psi$ . The clearest pattern in the estimates is that the mode in each treatment is to exaggerate in the direction of the bias: 83 percent of subjects in R(0) have an estimated exaggeration direction within a  $\frac{\pi}{36}$  radian cone of the bias direction, where this figure is 50 percent in R(.6) and 46 percent in R(1). However, a secondary pattern is the proportion with estimates counterclockwise from the bias in rotated treatments—a third of subjects in R(.6) and just under a half in R(1).

Despite the good fit in terms of the direction (*Restriction C*), the magnitudes of the off-ray exaggerations components are not negligible, and so we cannot accept *Restriction B* at face value. Sample-average magnitudes for residuals,  $\hat{\mathbb{E}} |\epsilon_{it}(\hat{\omega})|$ , are listed in Table SM-I, where *Restriction B* implies this number is at the boundary, with zero variation.<sup>4</sup> The exaggeration strategy makes

<sup>3</sup>Exaggerations from sender  $Y$ ,  $\tilde{y}_{it}$ , are reflected through the line passing through the origin and the average bias  $\frac{1}{2}(\delta^X + \delta^Y)$  to produce an effective exaggeration  $\tilde{x}_{it}$ . The symmetric  $Y$  exaggeration direction is therefore given by  $\gamma^Y(\omega) = \begin{pmatrix} \cos(\psi - \omega) & \sin(\psi - \omega) \end{pmatrix}'$ , the reflection of  $\gamma^X(\omega)$ .

<sup>4</sup>Allowing for subject-level variation in the exaggeration direction does not lead to large drops in the expected off-ray residuals. Within the rotated treatments R(.6) and R(1), subject-level heterogeneity in the exaggeration direction accounts for 3 percent and 9 percent, respectively, of the observed magnitudes  $\hat{\mathbb{E}} |\epsilon_{it}(\hat{\omega})|$ .

TABLE SM-I. Sender Estimates

Variable	R(0)	R(.6)	R(1) <sup>†</sup>
Exaggeration angle, $\hat{\omega}$	0.000 (0.000,0.000)	0.009 (0.000,0.021)	0.034 (0.018,0.058)
Ray exaggeration, $\hat{\mathbb{E}}\hat{\kappa}_{it}$	49.0° (-60.0, 134.0)	57.8° (-24.6, 142.3)	79.2° (-32.7, 179.8)
Error magnitude, $\hat{\mathbb{E}} \epsilon_{it}(\hat{\omega}) $	8.3° (0.0, 52.0)	14.8° (0, 56.3)	23.0° (0.0, 86.0)
$\zeta_{\hat{\Gamma}}(\mathbf{x}, \mathbf{y})$ parameters, $(\alpha, \beta_1, \beta_2)$	(1.00,0.00,0.00)	(0.74,0.45,0.43)	(0.50,0.54,0.47)
Attainable efficiency, $\Upsilon_S$	88.4%	81.4%	71.5%
Loss from <i>Restriction B</i> , $\tilde{\Upsilon}_S - \Upsilon_S$	8.4%	10.0%	9.2%

Note: 95 percent confidence intervals below the  $\hat{\omega}$  estimate are calculated using a bootstrap of size 1,000; confidence intervals below  $\hat{\kappa}$  and  $|\hat{\epsilon}|$  reflect 95 percent coverage for residuals under  $\hat{\omega}$  (two-sided for  $\kappa$ , one-sided for  $|\hat{\epsilon}|$ ). <sup>†</sup>R(1) estimates include data from 24 subjects in the first part of treatment E(1).

a very specific restriction, and a direct test of it is binary, *all* data either satisfies the restriction or the restriction fails. This is similar to results in choice, where *any* observed cycles in revealed preference lead to a falsification of rationality. In large datasets, such violations are almost always present, and the analysis switches to quantification of the degree of the violations. Our approach will be similar, where we will add the possibility of noise, and measure the effect of this noise against a benchmark.

Allowing for noise requires some pre-specification of the scale of this noise, so that a test might assess the probabilities the data is produced by this data generation process. Because of this we focus on criteria rather than statistical tests (much as principal component analysis does). Given our paper's aim, a useful way to understand the magnitudes of the departure from linear exaggeration, is through the effect on a receiver who believes that *Restriction B* holds, and by Proposition 1 follows a linear response. For example, in R(0), a receiver following the linear best-response to senders' exaggerations (identical to the equilibrium response here) would expect to have a final choice 8.3° distant from the true state in each issue, or, given the payoffs, a monetary loss of \$2.50.

Moreover, to facilitate comparisons with the receiver analysis in the paper's section 4.2, we will show how deviations from *Restriction B* affect the attainable efficiency with the *Proposition 1* response by receivers. Given the best-fit exaggeration directions, the exaggeration basis  $\hat{\Gamma} = [\gamma^X(\hat{\omega}) \quad \gamma^Y(\hat{\omega})]$ , the sequentially rational response  $\zeta_{\hat{\Gamma}}(\mathbf{x}, \mathbf{y})$  is summarized by three parameters,  $(\alpha, \beta_1, \beta_2)$ , which we list in Table SM-I. The efficiency level attainable given this response is

$$\Upsilon_S = 1 - \frac{\hat{\mathbb{E}}_{(\tilde{\mathbf{x}}, \tilde{\mathbf{y}})} \left\| \zeta_{\hat{\Gamma}}(\tilde{\mathbf{x}}, \tilde{\mathbf{y}}) \right\|}{\mathbb{E} \|\boldsymbol{\theta}\|},$$

where  $\hat{\mathbb{E}}_{(\tilde{\mathbf{x}}, \tilde{\mathbf{y}})} \left\| \zeta_{\hat{\Gamma}}(\tilde{\mathbf{x}}, \tilde{\mathbf{y}}) \right\|$  is the sample-average distance between  $\zeta_{\hat{\Gamma}}$  and the true state, assessed across all treatment exaggeration pairs  $(\tilde{\mathbf{x}}, \tilde{\mathbf{y}})$ , and  $\mathbb{E} \|\boldsymbol{\theta}\|$  is the analytical receiver choice distance

in a babbling equilibrium. This measure incorporates the deviations from linear exaggerations, and illustrates the efficiency attainable by a receiver following the Proposition 1 sequentially rational response.

The efficiency measure  $\Upsilon_S$  is listed by treatment in Table SM-I. The \$2.50 expected loss from noise in R(0) is mirrored as an 11.6 percentage point efficiency loss. In R(.6) and R(1) the increased magnitude for residuals translate to increased efficiency losses, 18.6 and 28.5 percent, respectively (with expected monetary losses to the receivers of \$4.19 and \$6.13). The effects from sender deviations from the linear restriction are substantial, and by comparing the  $\Upsilon_S$  measure to the observed efficiency measure  $\Upsilon$  listed in Table II in the paper, we can infer that this noise in sender behavior accounts for a slightly less than half of the final efficiency losses in each treatment.

However, we argue that though there are efficiency losses from sender deviations from *Restriction B*, the extent to which receivers can do better with more sophisticated beliefs is small. To make this case we compare the efficiency attainable under the linear exaggeration restriction ( $\Upsilon_S$ ) to an unrestricted *non-parametric* best response ( $\bar{\Upsilon}_S$ ). The unrestricted best response is

$$\bar{\zeta}(\mathbf{x}, \mathbf{y}) = \arg \min_{\mathbf{z}} \hat{\mathbb{E}}_{\tilde{\mathbf{x}}, \tilde{\mathbf{y}}} \left( \|\mathbf{z} - (\mathbf{x} - \tilde{\mathbf{x}})\| \mid \tilde{\mathbf{y}} - \tilde{\mathbf{x}} = \mathbf{y} - \mathbf{x} \right),$$

where we calculate expectations by simulation from the empirical distributions for  $\tilde{\mathbf{x}}$  and  $\tilde{\mathbf{y}}$ . Given  $\bar{\zeta}(\mathbf{x}, \mathbf{y})$  we calculate the upper bound on efficiency given senders' response

$$\bar{\Upsilon}_S = 1 - \frac{\hat{\mathbb{E}}_{(\tilde{\mathbf{x}}, \tilde{\mathbf{y}})} \left\| \bar{\zeta}(\tilde{\mathbf{x}}, \tilde{\mathbf{y}}) \right\|}{\mathbb{E} \|\boldsymbol{\theta}\|}.$$

The last row in Table SM-I provides the efficiency loss from maintaining *Restriction B*, the difference  $\bar{\Upsilon}_S - \Upsilon_S$ . In each of our treatments, receivers best responding to the assumption of linear exaggerations lose approximately ten percentage points from the attainable efficiency.

## APPENDIX C. ROBUSTNESS OF RECEIVER UNIDIMENSIONAL RESPONSE

A prominent result from comparing treatments R(0)–R(1) is subjects’ failure to use across-issue information. To examine this result we conduct two robustness exercises. The first changes the graphical interface used within the experiment, and seeks to understand whether the presentation, which had subjects make separate decisions in each issue rather than jointly, might be producing the across-issue failures. The second exercise provides extra opportunities for subjects to learn the across-issue response. It also increases the statistical power to estimate the subject-level response, doubling the number of rounds each subject plays as a receiver. For both exercises the evidence indicates that the findings we reported above are not qualitatively changed.

**C.1. Plane Interface.** In our R(·) treatments, receivers make separate choices in each issue. The graphical environment presents recommendations on two separate circles, and the final choice is made by clicking in each in turn. It is possible that the strategic connections between issues are more readily understood when recommendations are presented jointly, and receivers make one multidimensional choice. Our first robustness exercise seeks to understand whether receivers integrate across-issue information when the geometric connection between issues is clearer. To address this concern we conducted two additional treatments, denoted P(0) and P(1), with exactly the same underlying strategic structure as R(0) and R(1), respectively. The only change is the graphical interface in the experiment. Instead of depicting states/recommendations/choices as angles on two separate circles, the interface depicts them as points on a two-dimensional square. The interface is similar to a Cartesian representation of a globe, where our graphical interface shows the toroidal state-space’s fundamental polygon—opposed edges of the square are identified with one another. Choices for both senders and receivers in P(0) and P(1) are therefore inherently multidimensional, with receivers viewing senders’ recommendations (bias directions) as points (vectors) on the plane.<sup>5</sup>

We conducted two sessions each of P(0) and P(1), recruiting 15 new subjects for each session. Procedures were nearly identical to the previous sessions, with the exception that the projected instruction presentation and subjects’ instruction interface reflected the new interface.

Results from the two treatments P(0) and P(1) mirror our findings in R(0) and R(1), where we provide comparable figures to the R(·) treatments in Appendix D. Subjects use strategies as senders that are qualitatively close to *Restrictions A* and *B*, with a majority of subjects exaggerating in their bias direction, per *Restriction C*. As receivers, subjects perform very well in the P(0) treatment, with approximately half of the subjects mirroring the sequentially rational response. However, receiver subjects in P(1) again fare badly, and the two treatments are stochastically ordered, so that final efficiency distributions satisfy  $\Upsilon(P(0)) \succ_1^* \Upsilon(P(1))$ .<sup>6</sup> Examining subjects’ receiver response we see the same patterns: strategic thinking within the horizontal and vertical coordinates presented (averaging/shading), but subjects continue to treat the issues independently, as if solving each coordinate in isolation.

---

<sup>5</sup>The interface initially centers the square on the point (180,180), and allows subjects to recenter on any coordinate, any number of times, by right-clicking with their mouse. Instructions for these additional treatments, which include extensive screenshots are included in the online appendices.

<sup>6</sup>Subjects actually do better in R(0) than P(0), and  $\Upsilon(R(0)) \succ_1^{**} \Upsilon(P(0))$ , so the separation of issues might actually be beneficial. However, a similar exercise examining receiver’s distance from the sequentially rational response (receiver efficiency) indicates that the difference in efficiency is due to greater noise in sender recommendations within P(0). In comparison, we find no significant first-order stochastic relationships between  $\Upsilon(R(1))$  or  $\Upsilon(P(1))$ , nor indeed the extended treatment  $\Upsilon(E(1))$  we detail below.

**C.2. Extended Treatment Analysis.** Though many receiver subjects in our experiments do well through a non-linear, *within-issue* response, such response cannot be part of an equilibrium outcome in R(6) and R(1). In particular, any response by receivers that chooses a midpoint strictly between the within-issue recommendations provides an incentive for greater exaggeration by senders. Matching this idea, greater noise in the R(1) exaggerations is at least partly due to some sender subjects exaggerating more in the opposed-sign issues, where receivers response is a simple average. For the FRE to succeed in the long-run, it must be that receivers learn to incorporate across-issue information. To examine whether greater experience might lead to across-issue inferences, our second robustness exercise increases the number of periods subjects act as a receiver in part two of the session, while holding constant the senders' response.

We ran two further sessions (recruiting 24 subjects), for an extended version of R(1), which we label E(1). Subjects in E(1) followed identical procedures to R(1) in the first fifteen rounds—as such we incorporate the sender data into our R(1) analyses.<sup>7</sup> The difference in treatment came in the second part of the E(1) sessions. Instead of five rounds where all subjects are receivers (facing states/recommendations from the same session) we ran the second part for 15 rounds, using state/recommendation data randomly chosen (without replacement) from rounds 11–15 in the three previous R(1) sessions. Because data came from previous sessions, all 24 subjects in both E(1) sessions made choices  $\mathbf{z}_{it}$  in reaction to an identical sequence of underlying states and recommendations,  $\{\boldsymbol{\theta}_t, \mathbf{x}_t, \mathbf{y}_t\}_{t=16}^{30}$ .

In the E(1) treatment the set of subjects  $\mathcal{I}$  has 24 members. As a first approach we perform the same within-issue exercise as section 4.3, and classify 14 of the 24 subjects as taking a midpoint in issue 1 (the opposed issue) and shading from the minimal recommendation in issue 2 (the aligned issue). We partition the set of subjects into two subgroups, where  $\mathcal{W}$  captures the classified subjects and those unclassified are in  $\mathcal{I} \setminus \mathcal{W}$ .<sup>8</sup>

For each round  $t$ , let the median subject in subgroup  $\mathcal{G}$ 's efficiency level be  $\Upsilon_{.5}^t(\mathcal{G})$ . Table SM-II provides averages for the median subject's efficiency in each group across all rounds, and across blocks of five rounds in the first four columns. Before we discuss the figures in the table we make a few observations that will be useful to assess the evolution of efficiency levels. Because all 24 subjects in E(1) faced the common state/recommendation sequence  $\{\boldsymbol{\theta}_t, \mathbf{x}_t, \mathbf{y}_t\}_{t=16}^{30}$ , the selected order for the sequence may itself have an effect in the way that median efficiency evolves. Contrarily, in the last five rounds of R(1) subjects faced information from earlier rounds of the experiment in a random order. Consequently, as a reference, the last two columns of the table provide the median efficiency and interquartile range for the 45 subjects in the R(1) treatment, averaged over rounds 16–20.

Inspecting the three columns that show the five round blocks, there seems to be an increasing efficiency level. Moreover, breaking the analysis up to look at the subgroups  $\mathcal{W}$  and  $\mathcal{I} \setminus \mathcal{W}$ , it is clear that the increasing efficiency is primarily driven by subjects in the former subgroup, as the median subject in  $\mathcal{I} \setminus \mathcal{W}$  has a decreasing efficiency level across the blocks. However, the data

<sup>7</sup>We do not find any statistical differences between the E(1) sessions and R(1) sessions in the first 15 rounds with respect to senders' and receivers' choices.

<sup>8</sup>The classification is somewhat forgiving, allowing for an averaging parameter  $\hat{\alpha}_i \in (0.4, 0.6)$  in issue 1, and a shading parameter  $\hat{\eta}_i \leq 0$  in issue 2. This means that we exclude those following averages in issue 2. We require both issues to have a model-fit of  $R_i^2 > 0.6$ . We motivate the model-fit requirement by examining the parameters  $\alpha_i$  and  $\eta_i$  (and the corresponding  $R_i^2$ ) that the subjects followed the equilibrium response,  $\zeta^*(\mathbf{x}_{it}, \mathbf{y}_{it})$ . The equilibrium response, when estimated through a (mis-specified) within-issue response attains an  $R^2$  of 0.84 in issue 1 with an estimate  $\alpha = 0.48$ , in issue 2 the estimated parameter is  $\eta = -57.5$ , with a model  $R^2$  of 0.88.

suggest that the improvement in efficiency is not related to subjects making a connection across dimensions, but is rather an outcome of the particular sequence that subjects faced in E(1). First, if the random variation in R(1) and E(1) are comparable, the expected efficiencies will be centered at 48.3 percent. However, the final column illustrates the interquartile range for the 5-rounds efficiency averages in R(1), showing substantial variation across subjects, even were that subject to follow the equilibrium response. Observed increases could simply be the product of the specific sequence randomly chosen for E(1). To control for this variation more carefully, we will examine two counterfactuals, and compare subject’s results to these baselines.

The first counterfactual is our proxy for a within-issue strategy:

$$\bar{\zeta}(\mathbf{x}, \mathbf{y}) = \left( \zeta_{\text{Avg}}(x_1, y_1; \alpha = \frac{1}{2}) \quad \zeta_{\text{Min}}(x_2, y_2; \eta = -45) \right)'.$$

That is, choose midpoint in issue 1, and subtracts  $45^\circ$  from the minimal recommendation in issue 2. The second counterfactual computes the equilibrium response  $\zeta^*(\mathbf{x}_t, \mathbf{y}_t)$ , which incorporates across-issue information according to the equilibrium strategy. Table SM-II provides the efficiency levels these two counterfactual strategies would produce given the precise sequence of states/recommendations in E(1). Both strategies yield large increases across the three blocks of five rounds, with the equilibrium strategy doing somewhat better. Controlling for the information available, it seems that subjects actually do worse as the session evolves: in the first block subjects in  $\mathcal{W}$  do slightly better than the within-issue strategy  $\bar{\zeta}(\mathbf{x}, \mathbf{y})$ , but are doing worse than this baseline in the final two blocks of five. A better comparison can be obtained by dropping the two most extreme efficiency outliers from the first and last blocks. Examining rounds 18, 19 and 20 in the first block, and comparing this to rounds 28, 29 and 30 in the last block, the within-issue strategy yields an efficiency of 64 percent across 18–20, and 66 percent over 28–30 (the equilibrium strategy yields 80 percent and 75 percent, respectively). The median subject in  $\mathcal{W}$  (and in  $\mathcal{I} \setminus \mathcal{W}$ ) achieves 71 percent (31 percent) efficiency across 18–20, but just 61 percent (4 percent) in rounds 28–30. We therefore conclude that there is not compelling evidence for substantial improvement in subjects’ final *outcomes* as E(1) proceeds, that if anything, the evidence suggests decreases.

Despite subjects not improving their final outcomes, it might be that the observed drops stem from subjects beginning to incorporate across-issue information, albeit too coarsely. Our focus now will be on tests for whether subjects use across-issue information, which we construct using the differences between their choices and the two counterfactual responses outlined above. To motivate this comparison, Figure SM-1 illustrates three rounds in E(1) where the differences are pronounced. In each of the three plots, the exaggerations of the two senders  $\tilde{\mathbf{x}}_t$  and  $\tilde{\mathbf{y}}_t$  are illustrated as gray and white points, respectively. Each subject’s chosen point as the receiver ( $\tilde{\mathbf{z}}_{it} = \mathbf{z}_{it} - \boldsymbol{\theta}_t$ ) is labeled with the numbers 1–24, where black numbers indicate subjects in  $\mathcal{W}$ , white numbers in  $\mathcal{I} \setminus \mathcal{W}$ . Finally, each plot illustrates the two counterfactual decisions: i) the fully-revealing equilibrium choice  $\zeta^*(\mathbf{x}_t, \mathbf{y}_t) - \boldsymbol{\theta}_t$ , depicted as the black point; and ii) the within-issue strategy  $\bar{\zeta}(\mathbf{x}_t, \mathbf{y}_t) - \boldsymbol{\theta}_t$  depicted as the midpoint of a line interval, representing issue-2 shading strategies with  $\eta \in [-90, 0]$ .

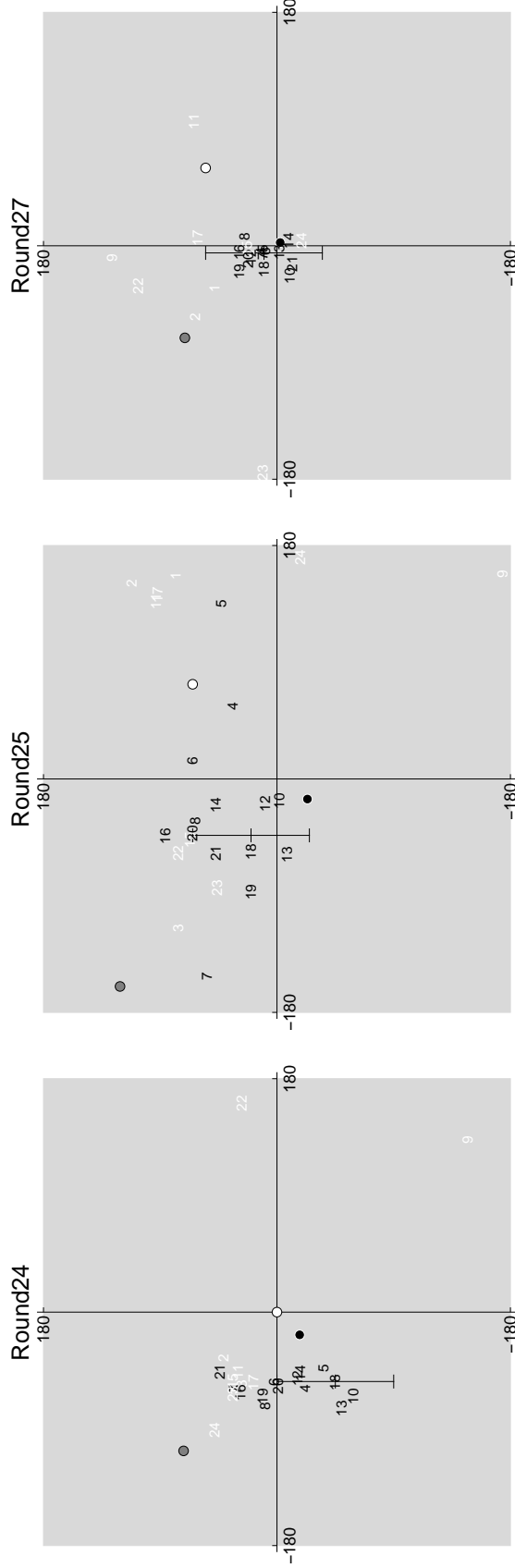
The third graph in the figure illustrates round 27, where the senders’ exaggerations have approximately the same magnitude. In this round both the within-issue and equilibrium strategies do well, attaining 92 and 97 percent efficiency, respectively (indeed, we dropped round 27 as an outlier in the above discussion). Unsurprisingly, subjects in  $\mathcal{W}$  do very well here, with average efficiency levels of 86 percent, while subjects in  $\mathcal{I} \setminus \mathcal{W}$  attain an average efficiency of 42 percent.



TABLE SM-II. Efficiency Across each Block of Five Rounds

Efficiency, $\Upsilon$	Median	Median		Median, Interquartile Range		
	All Rounds	16–20	21–25	26–30	R(1)	R(1)
All Subjects, $\mathcal{I}$	51.8%	45.2%	48.6%	61.6%	48.3%	8.7%–71.7%
$\mathcal{W}$ -Subjects	59.8%	51.1%	57.5%	70.9%	64.3%	40.0%–77.2%
$\mathcal{I} \setminus \mathcal{W}$ -Subjects	29.0%	36.1%	28.2%	22.8%	30.0%	0.9%–67.5%
$\bar{\zeta}(\mathbf{x}, \mathbf{y})$	62.8%	48.5%	63.2%	76.7%	63.1%	43.2%–78.8%
$\zeta^*(\mathbf{x}, \mathbf{y})$	71.6%	60.6%	72.5%	81.7%	72.1%	49.2%–90.3%

*Note:* For the subjects in R(1), 18 are selected into the group  $\mathcal{W}$  out of the 45 in this treatment; due to variation of the messages/states selected for each subject in R(1) the figures for  $\bar{\zeta}(\mathbf{x}, \mathbf{y})$  and  $\zeta^*(\mathbf{x}, \mathbf{y})$  represent the median/interquartile range for the counterfactual strategy averaged over the five rounds.



**FIGURE SM-1. Subject Receiver Reactions, E(1)**

*Note:* The true state is normalized to the origin. Gray point indicates the equilibrium choice  $\zeta_{\Delta}(\tilde{x}_t, \tilde{y}_t)$ , numbers represent subject choices  $\tilde{z}_{it}$ , where numbers in black represent subjects in  $\mathcal{W}$ , and numbers in white those in  $\mathcal{I} \setminus \mathcal{W}$ . The black line indicates the  $\zeta_{\text{Within}}(\mathbf{x}, \mathbf{y})$  choice, for the family of shading parameters  $\eta \in [-90, 0]$ .

In comparison to the third plot, the first two illustrate rounds where the two senders have asymmetric exaggeration magnitudes (most easily seen in the issue-2 difference,  $\tilde{y}_2 - \tilde{x}_2$ ). In both cases sender  $Y$  has exaggerated by less, and the equilibrium strategy therefore skews towards  $Y$ 's recommendation in the issue 1. However, the first two plots also vary in the sum of the exaggerations (seen in the separation between senders in issue 1,  $\tilde{y}_1 - \tilde{x}_1$ ), with the first plot having a smaller separation. Because of the this variation in the across-issue difference, the equilibrium strategy in the first plot (round 24) shades less than the second plot (round 25).<sup>9</sup>

Examining the response in Figure SM-1, it is hard to distinguish a clear pattern of subject response favoring the equilibrium point over the within-issue strategy. In each of the three rounds the  $Y$  sender can be identified as exaggerating less by inspecting  $y_{2t} - x_{2t}$ , and the simplest pattern to look for is subjects clustered to the right of  $\bar{\zeta}(\mathbf{x}_t, \mathbf{y}_t)$ . From just these three rounds, there is little evidence for the majority of subjects locating in this direction.

Our formal tests for across-issue inference examine all fifteen rounds in the final part of E(1), and look for associations between subjects' deviations from the within strategy, given by  $\bar{\epsilon}_{it} := \mathbf{z}_{it} - \bar{\zeta}(\mathbf{x}, \mathbf{y})$ , and the differences predicted by incorporating across-issue information as the equilibrium does, given by  $\epsilon_t^* := \zeta^*(\mathbf{x}_t, \mathbf{y}_t) - \bar{\zeta}(\mathbf{x}, \mathbf{y})$ . For each subject  $i \in \mathcal{W}$  and issue  $j \in \{1, 2\}$ , we test a null hypothesis of statistical independence between  $\bar{\epsilon}_{jit}$  and  $\epsilon_{jt}^*$ , across rounds  $t = 16, \dots, 30$ .<sup>10</sup> Using a one-sided Goodman-Kruskal test—so that the alternative hypothesis specifies positive dependence—we reject independence for just two subjects in issue 1 (subjects 4 at the 10 percent level, and subject 14 at the 2 percent level) and four subjects in issue 2 (subject 16 at the 10 percent level, subjects 8, 12 and 18 at the 5 percent level).<sup>11</sup> There is some evidence then, that a minority of subjects begin to incorporate components of the available across-issue information. However, no subject shows a statistical relationship in both issues, with the closest being subject 14, for whom we can reject independence at the 15 percent level in issue 2. Examining just the final five rounds, 26–30, we can reject independence for four subjects in issue 1 (4, 8, 14 and 18) but we reject for no subject in issue 2.<sup>12</sup> Finally, we note that although a small minority does begin to adjust for across-issue inferences within their final choice, the precise level at which they do so is not close to the sequentially rational response.

#### APPENDIX D. ADDITIONAL RESULTS AND FIGURES

<sup>9</sup>The round 25 figure also indicates that larger separation between the two recommendations lead some subjects to choose the wrong issue 1 arc. That is, they choose the arc where the  $X$  sender is clockwise, and the  $Y$  sender counterclockwise. In addition, the figure illustrates the general finding that this type of mistakes is more commonly made by  $\mathcal{I} \setminus \mathcal{W}$  subjects.

<sup>10</sup>For subjects in  $\mathcal{I} \setminus \mathcal{W}$  the test produces spurious correlations, as the common differenced component  $\bar{\zeta}(\mathbf{x}_t, \mathbf{y}_t)$  does not provide a useful baseline against which to consider deviations.

<sup>11</sup>A Kendall's tau test rejects independence for the same subjects. Hoeffding's independence test (two-sided) rejects independence for two subjects in issue 1 (subject 4 and 12 at the 10 percent level, subject 14 at the 1 percent level), and fails to reject for all subjects in issue 2.

<sup>12</sup>This failure to reject in the second issue seems to be related to reduced variance in the second component of  $\epsilon_t^*$  in the last five rounds. All five final rounds have an *equilibrium response* adding between  $-70^\circ$  and  $-49^\circ$  to the minimal recommendation. In contrast, the previous five rounds, 21–25, have effective  $\eta$  ranging between  $-116^\circ$  and  $-17.5^\circ$ .

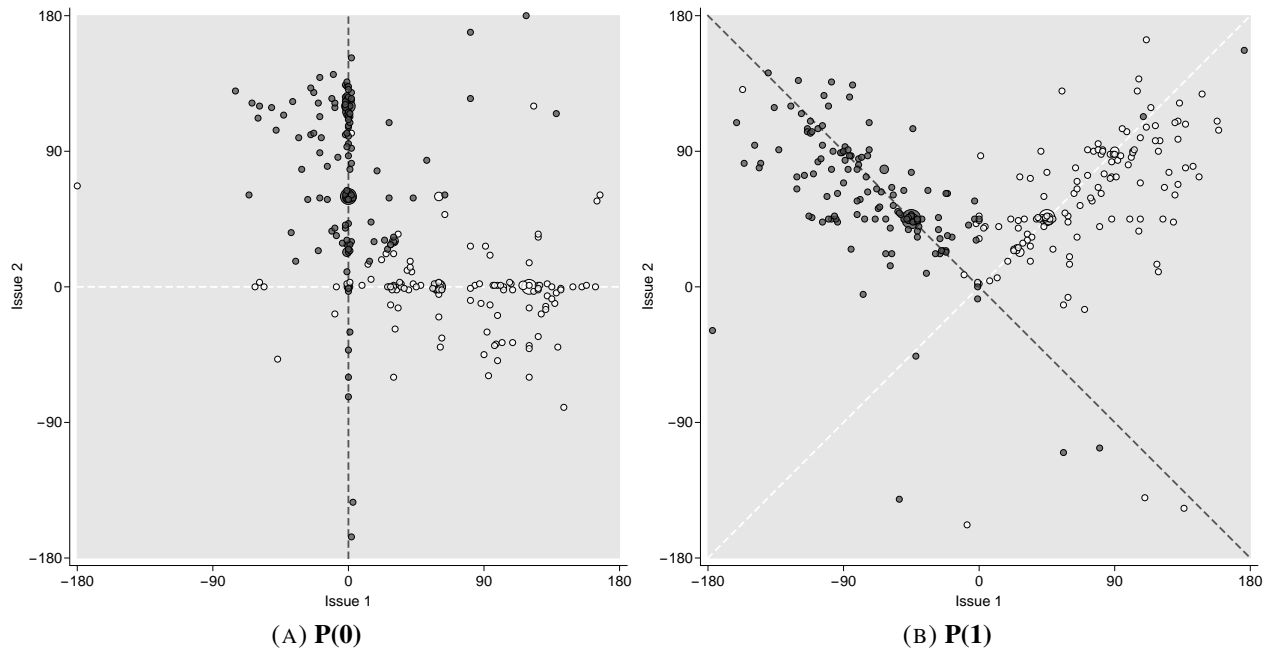


FIGURE D2. Sender Exaggerations

TABLE D3. Best Affine Receiver Strategy

	Receiver Strategy					
	Within Issue		Across Issue		Offset	
	$\bar{\alpha}_1$	$\bar{\alpha}_2$	$\bar{\beta}_1$	$\bar{\beta}_2$	$\bar{\eta}_1$	$\bar{\eta}_2$
<b>R(0)</b>	1.00	1.00	0.00	0.00	0.0	0.0
<b>R(.6)</b>	0.69	0.62	-0.43	-0.24	-2.9	-19.2
<b>R(1)</b>	0.48	0.52	-0.38	-0.24	-2.5	-25.7

*Note:* The strategies above minimize the expected choice error for a receiver using the following affine response

$$\zeta(\mathbf{x}, \mathbf{y}) = \begin{bmatrix} \alpha_1 & -\beta_1 \\ -\beta_2 & 1 - \alpha_2 \end{bmatrix} \begin{bmatrix} 1 - \alpha_1 & \beta_1 \\ \beta_2 & \alpha_2 \end{bmatrix} \begin{pmatrix} \mathbf{x} \\ \mathbf{y} \end{pmatrix} + \begin{pmatrix} \eta_1 \\ \eta_2 \end{pmatrix},$$

against the observed message pairs  $(\mathbf{x}, \mathbf{y})$ .

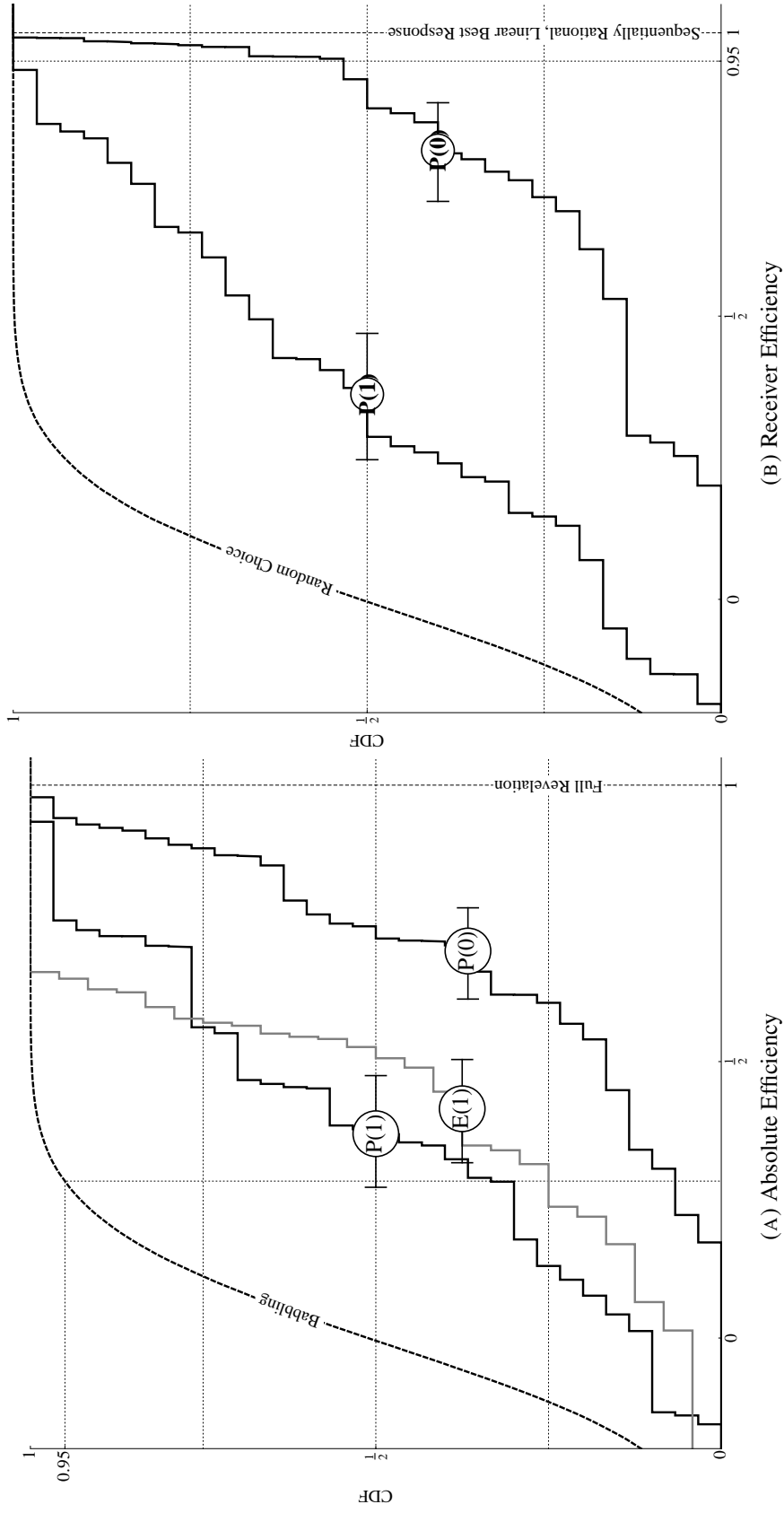
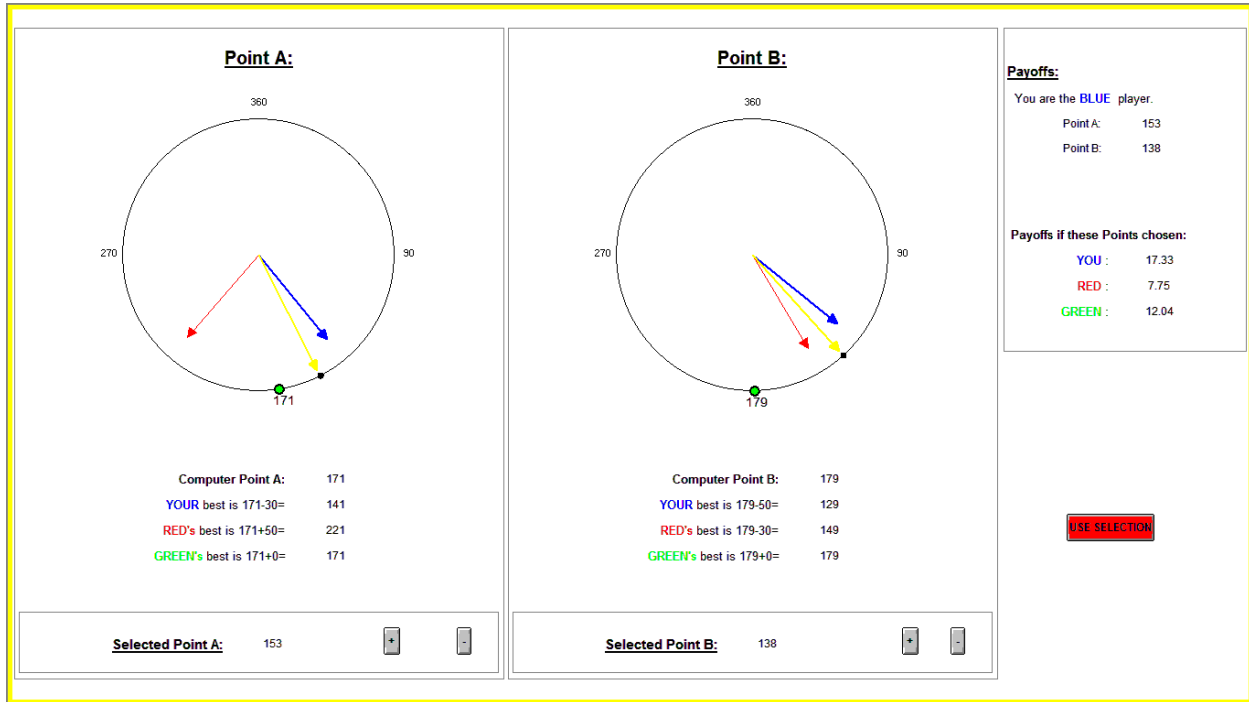
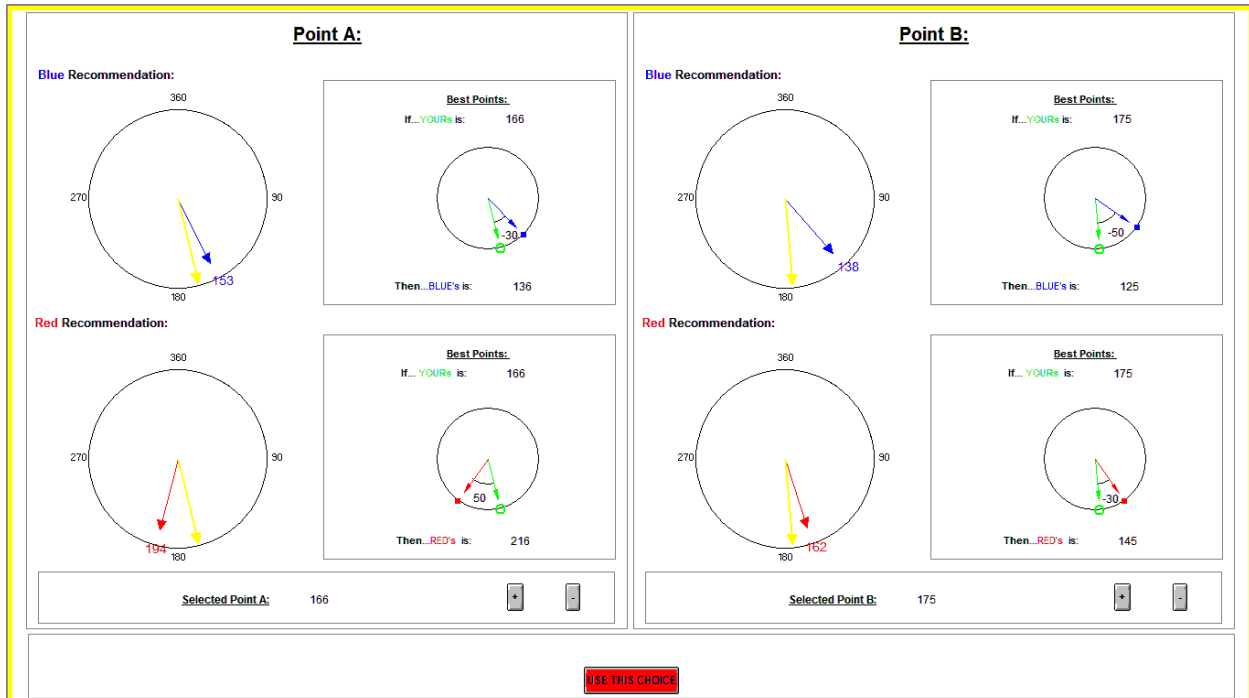


FIGURE D3. CDFs for subject's average decision efficiency

Note: Plot labels are located at the average efficiency level within the treatment; bars through the plot label represent the 95 percent confidence region for the distribution mean, extracted from a bootstrap.

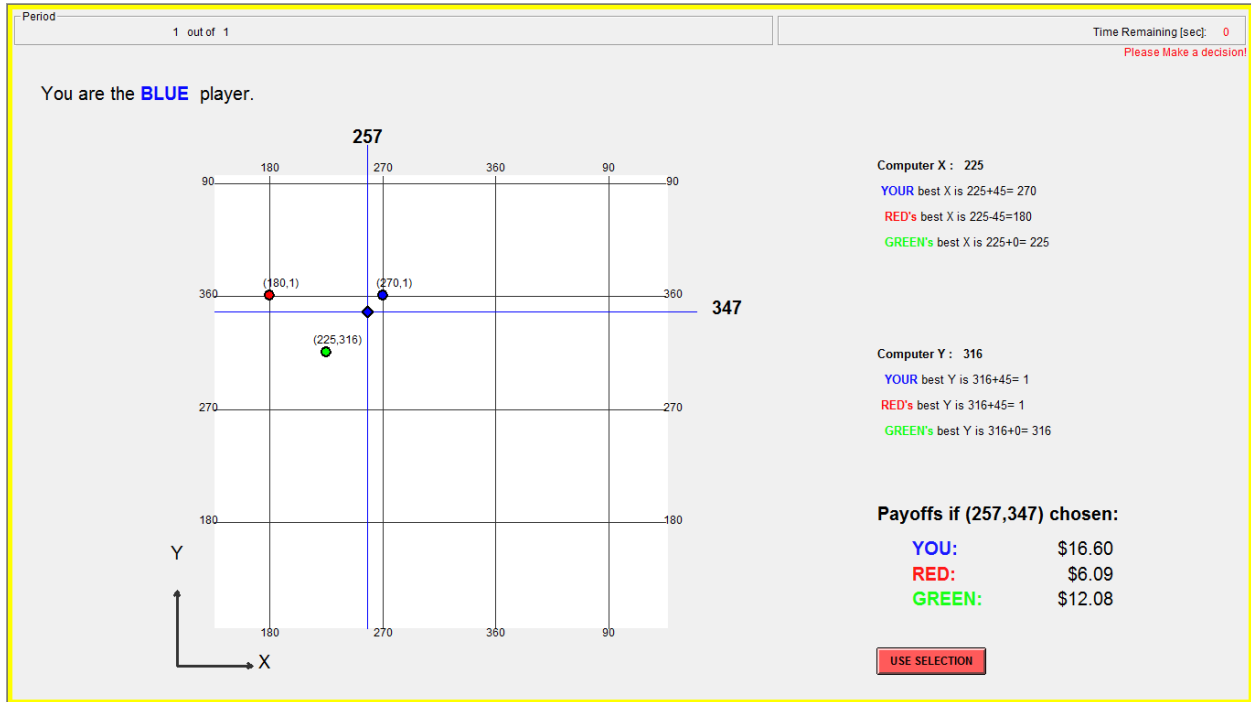


(A) Sender Interface

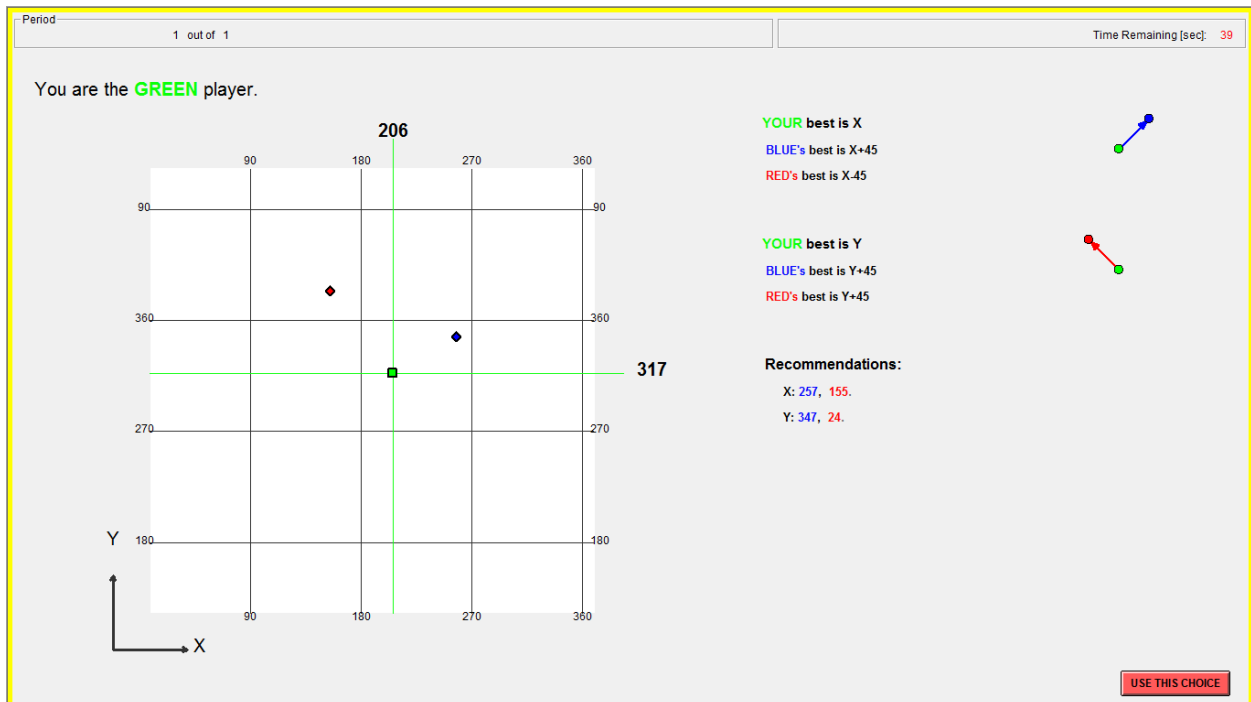


(B) Receiver Interface

FIGURE D4. Main Interface Screenshots



(A) Sender Interface



(B) Receiver Interface

FIGURE D5. Plane Interface Screenshots